MIT Libraries | DSpace@MIT

MIT Open Access Articles

Addressing Genetic Tumor Heterogeneity through Computationally Predictive Combination Therapy

The MIT Faculty has made this article openly available. ***Please share*** how this access benefits you. Your story matters.

Citation: Zhao, B., J. R. Pritchard, D. A. Lauffenburger, and M. T. Hemann. "Addressing Genetic Tumor Heterogeneity through Computationally Predictive Combination Therapy." Cancer Discovery 4, no. 2 (December 6, 2013): 166–174.

As Published: http://dx.doi.org/10.1158/2159-8290.cd-13-0465

Publisher: American Association for Cancer Research

Persistent URL: http://hdl.handle.net/1721.1/89180

Version: Author's final manuscript: final author's manuscript post peer review, without publisher's formatting or copy editing

Terms of use: Creative Commons Attribution-Noncommercial-Share Alike

Massachusetts Institute of Technology

NIH Public Access
Author Manuscript
Cancer Discov. Author manuscript; available in PMC 2014 August 01.

Published in final edited form as:
Cancer Discov. 2014 February ; 4(2): 166–174. doi:10.1158/2159-8290.CD-13-0465.

Addressing genetic tumor heterogeneity through computationally predictive combination therapy

Boyang Zhao[1,2], **Justin R. Pritchard**[2,3,*], **Douglas A. Lauffenburger**[2,3,4,*], and **Michael T. Hemann**[2,3,*]

[1]Computational and Systems Biology Program, Massachusetts Institute of Technology, Cambridge, MA 02139

[2]The David H. Koch Institute for Integrative Cancer Research, Massachusetts Institute of Technology, Cambridge, MA 02139

[3]Department of Biology, Massachusetts Institute of Technology, Cambridge, MA 02139

[4]Department of Biological Engineering, Massachusetts Institute of Technology, Cambridge, MA 02139

Abstract

Recent tumor sequencing data suggests an urgent need to develop a methodology to directly address intra-tumor heterogeneity in the design of anti-cancer treatment regimens. We use RNA interference to model heterogeneous tumors, and demonstrate successful validation of computational predictions for how optimized drug combinations can yield superior effects on these tumors both *in vitro* and *in vivo*. Importantly, we discover here that for many such tumors knowledge of the predominant subpopulation is insufficient for determining the best drug combination. Surprisingly, in some cases the optimal drug combination does not include drugs that would treat any particular subpopulation most effectively, challenging straightforward intuition. We confirm examples of such a case with survival studies in a murine pre-clinical lymphoma model. Altogether, our approach provides new insights concerning design principles for combination therapy in the context of intratumoral diversity, data that should inform the development of drug regimens superior for complex tumors.

Introduction

Recent high-throughput sequencing and genomic hybridization studies have revealed substantial intratumoral heterogeneity in cancer patients (1,2). Sections of single biopsies as well as biopsies taken from primary and metastatic regions revealed a highly complex nonlinear branching clonal evolutionary model as the basis for cancer progression and intratumoral diversity (3–11). Matched diagnostic and relapsed patient samples have also revealed the dynamic nature of a heterogeneous tumor, with the dominant subpopulation at relapse often originating from a minor pre-existing subclone (12–16). As such, spatial and temporal intratumoral heterogeneity presents a fundamental challenge for the rational design

[*]Corresponding authors: Michael Hemann, Massachusetts Institute of Technology, 77 Massachusetts Ave., 76-361B, Cambridge, MA 02139. Phone: (617) 324-1964; hemann@mit.edu; and Douglas Lauffenburger, Massachusetts Institute of Technology, 77 Massachusetts Ave., 16-343, Cambridge, MA 02139. Phone:(617) 252-1629; lauffen@mit.edu; and Justin Pritchard, Present address: Ariad Pharmaceuticals, 26 Landsdowne St., Cambridge, MA 02139. Phone: (617) 503-7511; justin.pritchard@ariad.com.

The authors declare no conflicts of interest related to this manuscript.

Author Contributions: B.Z., J.R.P., D.A.L. and M.T.H. designed research. B.Z. performed experiments and mathematical calculations. B.Z., J.R.P., D.A.L. and M.T.H. analyzed data. B. Z., D.A.L. and M.T.H. wrote the manuscript.

NIH-PA Author Manuscript
NIH-PA Author Manuscript
NIH-PA Author Manuscript

NIH-PA Author Manuscript

NIH-PA Author Manuscript

NIH-PA Author Manuscript

of combination chemotherapeutic regimens, which remain the primary treatment for most systemic malignancies.

There have been attempts to study heterogeneity and optimal therapeutic strategies. Many have been theoretical – on examining drug scheduling with generic single drugs or drug combinations on a heterogeneous population containing a sensitive and a resistant subpopulation (17–20). Some of these scheduling strategies have been followed by experimental validations *in vitro* (21,22). However, a rational approach to design drug combinations to minimize the effects of intratumoral heterogeneity in a tractable model with experimental validation *in vitro* and *in vivo* in preclinical models has been lacking.

Here we apply a computational optimization algorithm constructed on the experimental foundation of known single-drug efficacies for genetically variant cell subpopulations to predict how drug combinations will affect heterogeneous tumors. The most crucial assumption inherent in our algorithm has been demonstrated in our recent work: that commonly used combinations of chemotherapeutics act as linear averages of each component drug against homogenous tumors (23). For example, a two drug combination of drug A and drug B creates a combination selective pressure that resembles a simple weighted sum of A + B. Integration of this experimental foundation with our mathematical framework offers an advance in predictive understanding of how drug combinations influence the fate of heterogeneous tumors, which we successfully validated both *in vitro* and *in vivo*.

Results

RNAi-based approach to model heterogeneity and drug combination optimization

Our experimental system derives from the conceptual premise that tumors undergo branched clonal evolution with deregulated oncogene expression and/or tumor suppressor loss providing a basis for transformation, and additional genetic changes accumulating during tumor progression. These additional mutations underlie the development of a heterogeneous tumor population (Fig. 1A, as a simplified example). An attractive approach to model this heterogeneity in a tractable system amenable to systematic study is the use of an RNAi-based approach (Fig. 1B). Knockdown of specific genes of interest can approximate the loss of function that occurs in tumors, with the combination of multiple shRNA-expressing subpopulations modeling the diversity present in a heterogeneous tumor. We have previously used an RNAi-based approach to elucidate mechanisms of single and combination drug action (23,24) using *Eμ-myc; p19*$^{Arf-/-}$ lymphoma cells. Given this dataset of known therapeutic effects of cytotoxic and targeted therapies (Table S1) on individual shRNA-expressing subpopulations, we hypothesized that we could computationally predict superior versus inferior treatment strategies for minimizing subpopulations within a heterogeneous tumor (Fig. 1C).

Our mathematical algorithm is based on integer programming, which identifies the set of drugs that should be present in order to accomplish an aspired goal, or ‘objective function’. In the first manifestation here, the defined goal is to minimize outgrowth of specific tumor subpopulations within a known heterogeneous population (see Material and Methods and Supplementary Text for mathematical formulations). The rationale for this goal as a first test of our hypothesis is that current clinical approaches tend to focus on targeting the predominant tumor subpopulation, and the outgrowth of originally minor subpopulations representing resistance to that treatment is at present a daunting clinical problem.

We used this algorithm, in combination with a previously published dataset on drug-genotype interactions (23,24), to identify the most-effective two-drug combinations sampled

NIH-PA Author Manuscript

NIH-PA Author Manuscript

NIH-PA Author Manuscript

from a large number of three-component heterogeneous tumor populations (tumors that are comprised of two RNAi-produced sub-populations plus the parental sub-population) (Fig. S1). We then systemically simulated all possible combinations of three-component population and determined the most and least effective two-drug combinations (Table S2). In many cases, the optimal therapy was the same independent of whether we examined the entire heterogeneous population or just the predominate subpopulation. However, there was also a subset of population compositions where the solutions differ (Fig. S2). This suggests that for some heterogeneous tumor populations, we cannot derive the optimal therapy based on solely the predominant subpopulation alone. One such example was a three-component population consisting of the parental *Eμ-Myc; p19*$^{Arf-/-}$lymphoma (no shRNA) and subpopulations expressing either a Chk2 (a DNA damage checkpoint regulator) or a Bok (a Bcl2-family cell death mediator) shRNA. The optimal treatment for this tumor was a vincristine (Vin) plus SAHA combination, whereas the worst was an irinotecan (IRT) plus chlorambucil (CBL) combination. Interestingly, if only shChk2 or shBok populations were examined alone, the predicted optimal combination was neither Vin/SAHA nor IRT/CBL (Fig. 1D). Furthermore, SAHA was not the best single-agent for either shChk2 or shBok alone, but becomes part of an optimal drug combination in a heterogeneous population containing both shChk2 and shBok. This was also the case in examining lymphomas containing an alternative population composition of parental/shChk2/shBim. Thus, consideration of a heterogeneous tumor in its entirety can result in nonintuitive optimal drug combinations, sometimes containing drugs that are not the best single-agent for any subpopulations.

In vitro validation of drug combination on heterogeneous tumor

To experimentally validate these predictions, we used an *in vitro* fluorescence-based competition assay (Fig. 2A-B and Fig. S3), in which a mixture of parental lymphoma cells and shRNA-expressing subpopulations were exposed to combinations of drugs at controlled doses. Specifically, the drug combinations were dosed such that each drug in the combination contributed equally to a cumulative LD80-90 combination cell killing. GFP- or Tomato-labeled subpopulations enabled us to track the enrichment or depletion of individual subpopulations in the population mixture. Here, we observed that Vin/SAHA effectively maximized the therapeutic response in shBok-containing tumor cells (i.e. enhanced the depletion of shBok-infected cells) while minimizing the selective outgrowth of populations of tumor cells expressing shChk2 (Fig. 2C, Fig. S4). In contrast, IRT/CBL strongly selected for the resistant shChk2 subpopulation, and the parental subpopulation remained sensitive to both combinations. Combination treatment with actinomycin D (ActD)/Erlotinib or Vin/CBL, which were predicted to be optimal treatments if shChk2 or shBok subpopulations were considered individually, were less effective than Vin/SAHA. These predictions were also validated in a different tumor with a distinct population composition (Fig. 2D, Fig. S4). Taken together, these data suggest that combination therapies can be tailored to effectively minimize the effects of a heterogeneous tumor population given some knowledge of the composite subpopulations and their responses to single drugs.

As tumors continuously evolve with the acquisition of new mutations, forming more complex hierarchical structures, we wondered whether we could extend our simple model to account for another layer of complexity. Here, we performed an additional knockdown in our existing subpopulations to form a heterogeneous population consisting of parental, shChk2 (alone), shBok (alone), and shChk2 *plus* shBok. We then examined the response of these cells to the same four combination therapies and observed that the results were consistent with our predictions, with the optimal therapy still Vin/SAHA (Fig. 2E and F, Fig. S4). We can also apply principal component analysis as a method for dimensionality reduction and visualization on the resulting population, as we have done previously for

NIH-PA Author Manuscript

NIH-PA Author Manuscript

NIH-PA Author Manuscript

single populations (25,26). We observed that the optimal drug combination effectively impacts the population composition towards the goal of eliminating the shRNA subpopulations (Fig. S5). Thus, for this limited set of tested cases, we have demonstrated successful prediction of effective therapeutic strategy design, by computational integration of the individual drug effects across known target subpopulations, which can produce non-intuitive outcomes.

In vivo validation of drug combination on heterogeneous tumor in preclinical lymphoma model

We next sought to validate our predictions *in vivo*. The murine *Eμ-Myc* lymphoma model (27,28) allows us to perform *ex vivo* transduction of tumor cells followed by transplantation into syngeneic immunocompetent recipient mice (Fig. 3A). Lymph node, thymus, and spleen are among several sites of tumor dissemination in both donor and recipient tumor-bearing mice. Using this model, we observed substantial intratumoral heterogeneity by *ex vivo* whole mouse fluorescence imaging (Fig. 3B and Fig. S6). However, when we then analyzed individual lymph nodes, thymus, and spleen of untreated mice using flow cytometry, we observed heterogeneity at the level of individual tumors (Fig. S7). To validate the therapeutic effects *in vivo*, we determined the optimal dose for each of the individual drugs to ensure there was comparable therapeutic effect on parental tumors from each component drug in the combination (Fig. S8). Using these doses, combination treatment with Vin/SAHA successfully minimized the emergence of any tumor subpopulation, while IRT/CBL enriched significantly for the intrinsic resistant shChk2 subpopulation (Fig. 3C-D). Since our combination therapies were optimized to minimize specific tumor subpopulations relative to the parental lymphoma cells, we also examined the tumor-free survival of mice with heterogeneous lymphoma tumor normalized to that of mice with homogeneous lymphoma tumor. Upon treatments, Vin/SAHA improved the relative tumor-free survival compared to IRT/CBL (Fig. 3E). Taken together with our *in vitro* results, these data suggest that we can apply a mathematical optimization approach to predict optimal therapeutic strategies for minimizing the emergence of genetically defined tumor component populations and impact the tumor-free survival of mice when presented with a heterogeneous instead of homogeneous tumor.

We further explored the comparison between Vin/SAHA and IRT/CBL on relative tumor-free survival in shChk2/shBok/parental tumors across wide ranges of subpopulation proportions. With a three-component population, all tumor compositions can be represented on a ternary plot, with each corner corresponding to a homogeneous population of a single component and any point within the plot corresponding to some specific composition mixture of the three components. We experimentally determined the tumor-free survival of mice with homogeneous tumor containing one of the three subpopulations for treatment with either of the combination regimens (Fig. S9 and S10). Using this information, we generated a descriptive model showing the efficacy difference between Vin/SAHA and IRT/CBL across all possible subpopulation proportions. We observed that introducing heterogeneity (shChk2 and/or shBok subpopulations) into the parental tumor, Vin/SAHA increasingly improves the relative tumor-free survival (Fig. 4A). We can also derive the comparison in terms of absolute tumor-free survival, to inform us of tumor compositions for which Vin/SAHA dominates over IRT/CBL (Fig. S11). In both cases, an example heterogeneous tumor composition (used for the competition assays above), which was not used in generating the model approximates well with the prediction described by the model.

Since our optimization model predicts the effect of drug combinations on the evolution of tumor composition, and our descriptive model approximates the efficacy difference between treatments at specified tumor composition, we can combine these models to examine drug

NIH-PA Author Manuscript

NIH-PA Author Manuscript

NIH-PA Author Manuscript

efficacy at multiple time points upon single or consecutive drug treatments. While both drug combinations have minimal effects on changes of tumor composition with empty vector controls (Fig. 4B), the drug treatments predictably affected the heterogeneous tumor (Fig. 4C) – landing at tumor compositions at relapse for which we can also now estimate the therapeutic efficacy comparisons for the next round of treatment. As pre-existing subclones prior to treatment may exist at extremely low frequencies in clinically observed cases, we also examined theoretically the dynamics of tumor heterogeneity with multiple rounds of combination therapy at different initial tumor compositions, including extremes such as 0.1% pre-existing shChk2 and shBok. Sequential IRT/CBL strongly selected for the shChk2 subpopulation whereas Vin/SAHA had less selective pressure on the subpopulations (Fig. S12). Thus, based solely on tumor heterogeneity dynamics (assuming no new induced resistance mechanisms), Vin/SAHA remains as a superior effective drug combination whereas after several rounds of IRT/CBL, the effectiveness of this drug can be dramatically reduced due to the outgrowth of shChk2 in becoming the dominant subpopulation.

Taken together, knowledge of the *in vitro* efficacy of single drugs on individual subpopulations has allowed us to optimize for a drug combination that minimizes the effects of heterogeneity and improves relative tumor-free survival. We combined additional *in vivo* efficacy data of the chosen drug combinations on individual subpopulations to approximate the *in vivo* therapeutic responses over wide ranges of tumor subpopulation proportions in a heterogeneous tumor. These two models enable the tracking of tumor trajectories upon single and multi-course treatments and examination of the effectiveness of subsequent treatment strategies at relapse(s).

Discussion

Starting with Peter Nowell's seminal 1976 paper on the clonal evolution of cancer (29), we have gradually gained the ability to monitor and deconvolute the step-wise alterations in cancer evolution that underlie intratumoral heterogeneity. Not only are distinct tumor sub-clones found to coexist within the same tumor regions (30,31), but analyses of biopsies in primary and metastatic tumor sites further suggests that metastatic sub-clones originate from a non-metastatic parental clone in the primary tumor (3–11). Additional changes at the post-transcriptional and epigenetic level can potentially further diversify a tumor population with functional variations (32,33). This heterogeneous tumor population is also dynamic, as has been shown in the responses to standard combination chemotherapeutic regimens, with pre-existing minor sub-clones expanding to dominate at relapse (12–16). As such, current combination regimens can have unpredictable and/or unintended consequences on the resulting tumor diversity. The original rationale for the use and choice of combination therapies has been primarily to increase the effective and tolerable drug dose, while minimizing resistance (34–38). In theory, this leads to more cancer cell killing and decreases the likelihood that a resistant clone will compromise therapeutic success. However, in light of recent studies showing the extent of intratumoral variation and its clinical implications, it is paramount to incorporate tumor diversity and the expected evolutionary trajectories into rational drug combination design to achieve predictable tumor response, reduce chances of relapse, and prolong patient survival. Our joint theoretical and experimental approach suggests that we can derive drug combinations that can minimize outgrowth of specific subpopulations in a given heterogeneous tumor while enhancing tumor-free survival in mice – provided we know some knowledge of the tumor composition and the response of component subpopulations to single drugs.

Here we used the *Eμ-Myc* lymphoma mouse model as the basis for our computational modeling and experimental validations. The presence of $p19^{Arf-/-}$ in this model may remove selective pressure on specific mutations that arise during tumor progression and in response

NIH-PA Author Manuscript

NIH-PA Author Manuscript

NIH-PA Author Manuscript

to treatment. Thus, the broad applicability of this approach to other cancer models remains to be seen. Nevertheless, the *Eμ-Myc* lymphoma model is an extremely well-characterized preclinical mouse model and thus a good initial system to tractably address the rational design of drug regimens in the context of genetically diverse tumor. Furthermore, *Eμ-myc* models a defining translocation observed in Burkitt's lymphoma. Previous targeted molecular analyses on different sites of the same patient and matched sample at diagnosis and relapse revealed shared *Myc* breakpoints and *Bcl-6* mutations, but differential *p53* and *Myc* mutations across the different samples, suggesting clonal evolution spanning across different tumor sites and in response to treatment (39).

The complexity of heterogeneous tumors found in patients undoubtedly complicates applications of this approach. However, our studies highlight basic principles towards rational drug combination design. For example, as was the case for Vin/SAHA in this tumor model, a therapeutic strategy may involve finding a set of drugs that, when combined, maximizes the therapeutic synthetic lethality of certain subpopulation(s), while minimizing the selective pressure for outgrowth of cells bearing undesirable alteration(s). Here, the maintenance of tumor heterogeneity – representing the persistence of a "naïve" pre-treatment state – may be preferable to the undesirable outgrowth of specific subpopulation(s). On the other hand, if we can potentially drive towards the enrichment of therapeutic sensitive subpopulations while preserving overall tumor sensitivity, a sequential treatment approach may be successful as part of a multi-course regimen. Thus, the ability to apply optimization approaches to control the trajectories of tumor composition offer opportunities to maximize the effects of concurrent or successive drug combination regimens.

Materials and Methods

Cell culture and chemicals

Murine *Eμ-myc; p19$^{Arf-/-}$* B-cell lymphomas were cultured in B-cell medium (45% DMEM, 45% IMDM, 10% FBS, supplemented with 2mM L-glutamine and 5μM β-mercaptoethanol). The cell line was tested and shown to be free of mycoplasma using both PCR-based (ATCC) and biochemical-based (Lonza) methods. All drugs were obtained from LC Laboratories, Sigma-Aldrich, Calbiochem, or Tocris Biosciences. For *in vivo* studies, irinotecan, chlorambucil, and vorinostat were dissolved in DMSO as stock and further diluted in 0.9% NaCl solution prior to injection. Vincristine was dissolved in 0.9% NaCl solution.

shRNA constructs

All shRNAs were expressed in either MSCV-LTR-MIR30-SV40-GFP (MLS) (40) or MSCV-LTR-MIR30-PGK-Tomato (MLT) retroviral vector and were previously validated for knockdown (24). Multiple shRNAs targeting each gene were used for single drug responses to rule out off-target effects (24). Transfection and transduction were performed as previously described (23).

In vitro competition assay

Single and combination drug treatments *in vitro* were performed as previously described (23,24) (see Fig. S3). Briefly, lymphoma cells were infected to ∼20% of the total population with the indicated retroviruses and were dosed with single or two drug combinations at concentrations needed to achieve 80-90% cell death (LD80-90) on the empty vector control (MLS or MLT) cells (assessed at 48 h). For combination treatments, each drug was dosed to ensure equal contribution of overall killing in the combination. Cell death was assessed with propidium iodide incorporation. Every 24 h, untreated and treated cells were diluted 1:4 and 1:2, respectively. At 72 h, the percentage of GFP+ and/or Tomato+ cells were analyzed on a

NIH-PA Author Manuscript

NIH-PA Author Manuscript

NIH-PA Author Manuscript

cell analyzer FACSScan, FACSCalibur, or LSRFortessa (BD Biosciences). To assess enrichment/depletion of the subpopulations, a log transformed Resistance Index (RI) (23,24) was calculated: $\log2RI = \log_2[(L_t - L_tL_u)/(L_u - L_tL_u)]$, where L_t and L_u represents percentage of labeled cells (GFP+ and/or Tomato+) out of the total live population with and without treatment, respectively. See Supplemental Text for derivations of log2RI. Experiments were performed with indicated shRNAs in both MLS and MLT vectors to rule out any vector-specific effects.

In vivo competition and survival assay

Two million infected *Eμ-myc; p19$^{Arf-/-}$* lymphoma cells were tail-vein injected into 7-9 weeks female syngeneic recipient C56/BL6 mice. Upon palpable tumor (~12-13 days after injection), mice were treated with single or combination drug regimens. Dosing for each drug was determined to ensure comparable efficacy on control uninfected lymphoma cells. Irinotecan (IRT) was administered at 120 mg/kg i.p. once on day 1; vincristine (Vin) at 1 mg/kg i.p. once on day 1; chlorambucil (CBL) at 10 mg/kg i.p. once on day 1; and vorinostat (SAHA) at 300 mg/kg i.p. on days 1 and 3 and 150 mg/kg on days 2 and 4. Vehicle control consisted of maximum equivalent doses of DMSO and 0.9% NaCl solution. For competition assay, lymphoma cells from thymus, lymph node, and spleen were harvested at sizable palpable tumor after relapse and analyzed on a cell analyzer. For survival studies, tumor-free survival was monitored by daily palpation following treatment.

In vivo fluorescence imaging

Fluorescence imaging of mice was acquired using the IVIS imaging system and Living Image software v4.3.1 (PerkinElmer). Two excitations (535nM and 465nM) with 9 emission filters (for a pairwise combination of ten) were used. GFP, Tomato, and background signals were spectral unmixed with resulting composite image further enhanced with brightness and contrast.

Mathematical optimization and models

The optimization of combination therapies for minimizing heterogeneous subpopulations was mathematically formulated as a binary integer programming problem. All analyses were performed in MATLAB R2012b (MathWorks). Binary integer programming was solved using the bintprog function in the MATLAB Optimization Toolbox. In determining cases for experimental validation, we sorted the simulation results based on difference in treatment effectiveness (evaluated by $\log_2$RI) between therapy optimized based on consideration of entire heterogeneity and that of just the predominant subpopulation. We validated cases with large efficacy differences, including non-intuitive cases (e.g. optimal drug combinations for heterogeneous that does not contain component drugs best for predominant subpopulation) and cases with different heterogeneous tumor compositions. Refer to Supplemental Text for more details on the mathematical model for optimization and descriptive model on the efficacy comparison between Vin/SAHA and IRT/CBL.

Rotated principal component analysis

Rotated principal component analysis was used to visualize the impact of different drug combinations on tumor composition. The data consists of a single matrix with each row representing a different treatment condition (or a pure subpopulation) and each column representing an averaged $\log_2$RI for each drug. The averaged $\log_2$RI was derived from matrix multiplication of the enrichment/depletion dataset matrix, **R** (see mathematical models section in Supplemental Text) by population composition vector, **p**, determined experimentally following treatment. Thus, the derived data represents a pharmacological profile for each resulting population following a specific treatment condition. The data was

NIH-PA Author Manuscript

NIH-PA Author Manuscript

NIH-PA Author Manuscript

mean centered and unit variance scaled. Principal component analysis (PCA) was performed using SIMCA-P v11.5 (Umetrics). For ease of interpretation, a linear transformation of the principal component space was performed using MATLAB by rotating the parental population projection completely into the second principal component.

Statistical analyses

Statistical analyses were performed using Prism v5 (GraphPad). Two-tailed Student's t-tests and one-way ANOVA (with Bonferroni post-hoc test) were used, as indicated. Error bars represent mean ± s.e.m. Logrank (Mantel-Cox) test was used for comparison of survival curves.

Supplementary Material

Refer to Web version on PubMed Central for supplementary material.

Acknowledgments

We thank Luke Gilbert and Peter Bruno for advice on experimental procedures; members of the Lauffenburger and Hemann lab for helpful discussions; and Peter Bruno, Eleanor Cameron, Miles Miller, and Aaron Meyer for comments on the manuscript. Funding was provided by Integrative Cancer Biology Program Grant U54-CA112967-06 (to M.T.H. and D.A.L.). B.Z. is supported by the NIH/NIGMS Interdepartmental Biotechnology Training Program 5T32GM008334. This work was also supported in part by the Koch Institute Support (core) Grant P30-CA14051 from the National Cancer Institute.

References

1. Swanton C. Intratumor Heterogeneity: Evolution through Space and Time. Cancer Res. 2012; 72:4875–82. [PubMed: 23002210]
2. Fisher R, Pusztai L, Swanton C. Cancer heterogeneity: implications for targeted therapeutics. Br J Cancer. 2013:1–7.
3. Anderson K, Lutz C, van Delft FW, Bateman CM, Guo Y, Colman SM, et al. Genetic variegation of clonal architecture and propagating cells in leukaemia. Nature. 2011; 469:356–61. [PubMed: 21160474]
4. Walter MJ, Shen D, Ding L, Shao J, Koboldt DC, Chen K, et al. Clonal architecture of secondary acute myeloid leukemia. N Engl J Med. 2012; 366:1090–8. [PubMed: 22417201]
5. Gerlinger M, Rowan AJ, Horswell S, Larkin J, Endesfelder D, Gronroos E, et al. Intratumor heterogeneity and branched evolution revealed by multiregion sequencing. N Engl J Med. 2012; 366:883–92. [PubMed: 22397650]
6. Yachida S, Jones S, Bozic I, Antal T, Leary R, Fu B, et al. Distant metastasis occurs late during the genetic evolution of pancreatic cancer. Nature. 2010; 467:1114–7. [PubMed: 20981102]
7. Campbell PJ, Yachida S, Mudie LJ, Stephens PJ, Pleasance ED, Stebbings L, et al. The patterns and dynamics of genomic instability in metastatic pancreatic cancer. Nature. 2010; 467:1109–13. [PubMed: 20981101]
8. Shah SP, Morin RD, Khattra J, Prentice L, Pugh T, Burleigh A, et al. Mutational evolution in a lobular breast tumour profiled at single nucleotide resolution. Nature. 2009; 461:809–13. [PubMed: 19812674]
9. Ding L, Ellis MJ, Li S, Larson DE, Chen K, Wallis JW, et al. Genome remodelling in a basal-like breast cancer metastasis and xenograft. Nature. 2010; 464:999–1005. [PubMed: 20393555]
10. Navin N, Kendall J, Troge J, Andrews P, Rodgers L, McIndoo J, et al. Tumour evolution inferred by single-cell sequencing. Nature. 2011; 472:90–4. [PubMed: 21399628]
11. Wu X, Northcott Pa, Dubuc A, Dupuy AJ, Shih DJH, Witt H, et al. Clonal selection drives genetic divergence of metastatic medulloblastoma. Nature. 2012; 482:529–33. [PubMed: 22343890]

NIH-PA Author Manuscript

NIH-PA Author Manuscript

NIH-PA Author Manuscript

12. Mullighan CG, Phillips LA, Su X, Ma J, Miller CB, Shurtleff SA, et al. Genomic analysis of the clonal origins of relapsed acute lymphoblastic leukemia. Science. 2008; 322:1377–80. [PubMed: 19039135]

13. Ding L, Ley TJ, Larson DE, Miller Ca, Koboldt DC, Welch JS, et al. Clonal evolution in relapsed acute myeloid leukaemia revealed by whole-genome sequencing. Nature. 2012; 481:506–10. [PubMed: 22237025]

14. Schuh A, Becq J, Humphray S, Alexa A, Burns A, Clifford R, et al. Monitoring chronic lymphocytic leukemia progression by whole genome sequencing reveals heterogeneous clonal evolution patterns. Blood. 2012; 120:4191–6. [PubMed: 22915640]

15. Keats JJ, Chesi M, Egan JB, Garbitt VM, Palmer SE, Braggio E, et al. Clonal competition with alternating dominance in multiple myeloma. Blood. 2012; 120:1067–76. [PubMed: 22498740]

16. Landau DA, Carter SL, Stojanov P, McKenna A, Stevenson K, Lawrence MS, et al. Evolution and Impact of Subclonal Mutations in Chronic Lymphocytic Leukemia. Cell. 2013; 152:714–26. [PubMed: 23415222]

17. Foo J, Michor F. Evolution of resistance to anti-cancer therapy during general dosing schedules. J Theor Biol. 2010; 263:179–88. [PubMed: 20004211]

18. Panetta JC. A mathematical model of drug resistance: heterogeneous tumors. Math Biosci. 1998; 147:41–61. [PubMed: 9401351]

19. Beckman RA, Schemmann GS, Yeang CH. Impact of genetic dynamics and single-cell heterogeneity on development of nonstandard personalized medicine strategies for cancer. Proc Natl Acad Sci U S A. 2012; 109:14586–91. [PubMed: 22891318]

20. Coldman AJ, Goldie JH. A stochastic model for the origin and treatment of tumors containing drug-resistant cells. Bull Math Biol. 1986; 48:279–92. [PubMed: 3828558]

21. Chmielecki J, Foo J, Oxnard GR, Hutchinson K, Ohashi K, Somwar R, et al. Optimization of dosing for EGFR-mutant non-small cell lung cancer with evolutionary cancer modeling. Sci Transl Med. 2011; 3:90ra59.

22. Das Thakur M, Salangsang F, Landman AS, Sellers WR, Pryer NK, Levesque MP, et al. Modelling vemurafenib resistance in melanoma reveals a strategy to forestall drug resistance. Nature. 2013; 494:251–5. [PubMed: 23302800]

23. Pritchard JR, Bruno PM, Gilbert LA, Capron KL, Lauffenburger DA, Hemann MT. Defining principles of combination drug mechanisms of action. Proc Natl Acad Sci U S A. 2013; 110:E170–9. [PubMed: 23251029]

24. Jiang H, Pritchard JR, Williams RT, Lauffenburger DA, Hemann MT. A mammalian functional-genetic approach to characterizing cancer therapeutics. Nat Chem Biol. 2011; 7:92–100. [PubMed: 21186347]

25. Janes, Ka; Albeck, JG.; Gaudet, S.; Sorger, PK.; Lauffenburger, Da; Yaffe, MB. A systems model of signaling identifies a molecular basis set for cytokine-induced apoptosis. Science. 2005; 310:1646–53. [PubMed: 16339439]

26. Cosgrove BD, Alexopoulos LG, Hang T, Hendriks BS, Sorger PK, Griffith LG, et al. Cytokine-associated drug toxicity in human hepatocytes is associated with signaling network dysregulation. Mol Biosyst. 2010; 6:1195–206. [PubMed: 20361094]

27. Adams JM, Harris AW, Pinkert CA, Corcoran LM, Alexander WS, Cory S, et al. The c-myc oncogene driven by immunoglobulin enhancers induces lymphoid malignancy in transgenic mice. Nature. 1985; 318:533–8. [PubMed: 3906410]

28. Schmitt CA, McCurrach ME, de Stanchina E, Wallace-Brodeur RR, Lowe SW. INK4a/ARF mutations accelerate lymphomagenesis and promote chemoresistance by disabling p53. Genes Dev. 1999; 13:2670–7. [PubMed: 10541553]

29. Nowell PC. The clonal evolution of tumor cell populations. Science. 1976; 194:23–8. [PubMed: 959840]

30. Szerlip NJ, Pedraza A, Chakravarty D, Azim M, McGuire J, Fang Y, et al. Intratumoral heterogeneity of receptor tyrosine kinases EGFR and PDGFRA amplification in glioblastoma defines subpopulations with distinct growth factor response. Proc Natl Acad Sci U S A. 2012; 109:3041–6. [PubMed: 22323597]

NIH-PA Author Manuscript

NIH-PA Author Manuscript

NIH-PA Author Manuscript

31. Snuderl M, Fazlollahi L, Le LP, Nitta M, Zhelyazkova BH, Davidson CJ, et al. Mosaic amplification of multiple receptor tyrosine kinase genes in glioblastoma. Cancer Cell. 2011; 20:810–7. [PubMed: 22137795]
32. Notta F, Mullighan CG, Wang JCY, Poeppl A, Doulatov S, Phillips La, et al. Evolution of human BCR-ABL1 lymphoblastic leukaemia-initiating cells. Nature. 2011; 469:362–7. [PubMed: 21248843]
33. Kreso A, O'Brien Ca, van Galen P, Gan OI, Notta F, Brown AMK, et al. Variable Clonal Repopulation Dynamics Influence Chemotherapy Response in Colorectal Cancer. Science. 2013; 339:543–8. [PubMed: 23239622]
34. Law LW. Origin of the resistance of leukaemic cells to folic acid antagonists. Nature. 1952; 169:628–9. [PubMed: 14929259]
35. Law LW. Effects of combinations of antileukemic agents on an acute lymphocytic leukemia of mice. Cancer Res. 1952; 12:871–8. [PubMed: 13009674]
36. Goldie JH, Coldman AJ. A mathematic model for relating the drug sensitivity of tumors to their spontaneous mutation rate. Cancer Treat Rep. 1979; 63:1727–33. [PubMed: 526911]
37. Goldie JH, Coldman AJ. The genetic origin of drug resistance in neoplasms: implications for systemic therapy. Cancer Res. 1984; 44:3643–53. [PubMed: 6744284]
38. Pinkel D, Hernandez K, Borella L, Holton C, Aur R, Samoy G, et al. Drug dosage and remission duration in childhood lymphocytic leukemia. Cancer. 1971; 27:247–56. [PubMed: 5100389]
39. Gutiérrez MI, Bhatia K, Cherney B, Capello D, Gaidano G, Magrath I. Intraclonal molecular heterogeneity suggests a hierarchy of pathogenetic events in Burkitt's lymphoma. Ann Oncol. 1997; 8:987–94. [PubMed: 9402172]
40. Dickins, Ra; Hemann, MT.; Zilfou, JT.; Simpson, DR.; Ibarra, I.; Hannon, GJ., et al. Probing tumor phenotypes using stable and regulated synthetic microRNA precursors. Nat Genet. 2005; 37:1289–95. [PubMed: 16200064]

NIH-PA Author Manuscript

NIH-PA Author Manuscript

NIH-PA Author Manuscript

Statement of Significance

This study provides the first example of how combination drug regimens, using existing chemotherapies, can be rationally designed to maximize tumor cell death, while minimizing the outgrowth of clonal subpopulations.

NIH-PA Author Manuscript

NIH-PA Author Manuscript

NIH-PA Author Manuscript

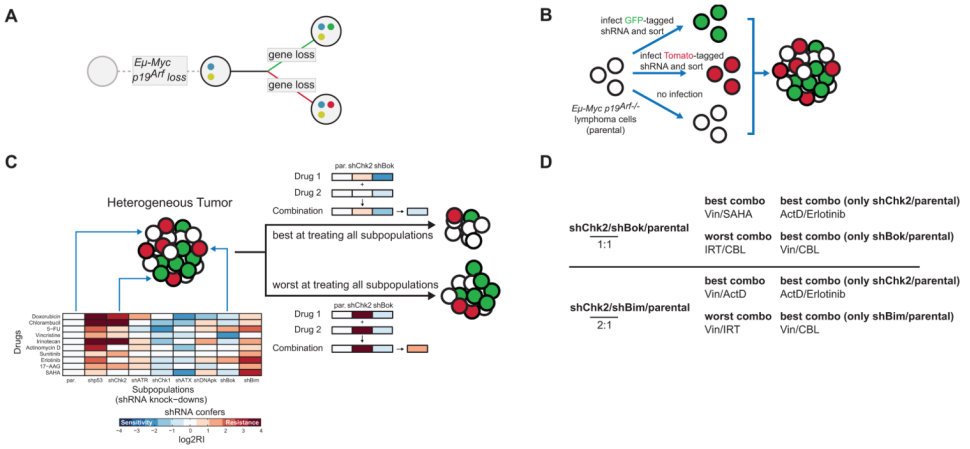

Fig. 1. A strategy for modeling intratumoral heterogeneity and mathematical optimization

(A) A simplified schematic of tumor evolution, with deregulated *Myc* expression and *p19*^{Arf} loss, followed by additional loss-of-function mutations. (B) RNAi-based modeling of intratumoral heterogeneity. Each shRNA knockdown models a specific loss-of-function event. Mixture of these subpopulations creates a heterogeneous tumor population. (C) A schematic of how mathematical optimization can be applied to drug design for tumor heterogeneity. We have previously acquired a dataset on the response of specific shRNA knockdowns to a set of single chemotherapeutic and targeted agents (23,24). Here, using this dataset and given a particular population composition, we applied an optimization approach (see Material and Methods) to determine drug combinations that are best and worst at treating all subpopulations. (D) Two top “hits” (i.e. population compositions) derived from computational simulation demonstrating that the optimal drug combination predicted is different depending on whether we examine the entire heterogeneous tumor population or only a particular subpopulation (see Fig. S2 and Table S1 for summary of all simulation results).

NIH-PA Author Manuscript

NIH-PA Author Manuscript

NIH-PA Author Manuscript

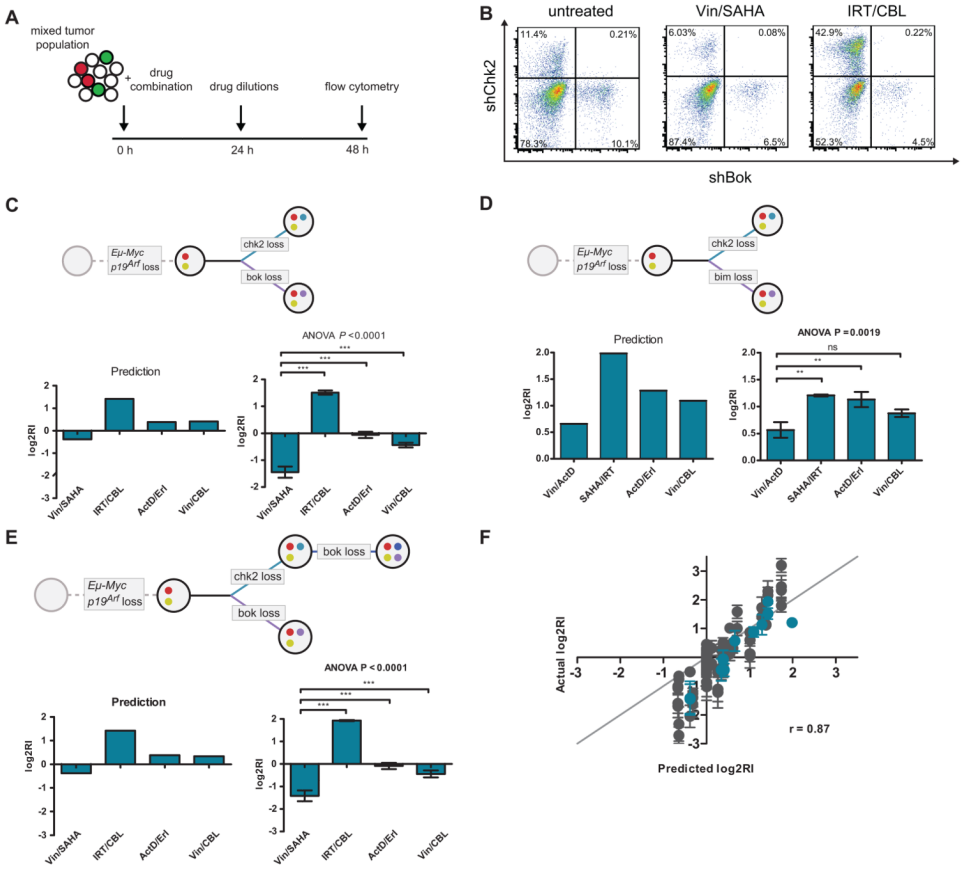

Fig. 2. *In vitro* validation of predicted effects of combination therapies on subpopulation composition

(A) A schematic of the *in vitro* competition assay (see also Fig. S3). *Eμ-Myc; p19*$^{Arf-/-}$ lymphoma cells were retrovirally transduced with the desired shRNA(s). Mixed populations were treated with combination treatment and analyzed at 48h. (B) A representative flow cytometry result of no treatment and the indicated combination treatments of a mixed population of tumor cells containing parental, shChk2 (Tomato-labeled), and shBok (GFP-labeled). (C-E) *In vitro* competition assay results for different population composition using different combination treatments. Drug combinations predictably enriched/depleted subpopulations. (F) Correlation between predictions made from mathematical model and the actual experimental results. Gray data points represent individual subpopulations (e.g. shChk2 only) and blue data points represent combined subpopulations (e.g. shChk2 and shBok). Data shown are mean ± s.e.m. of three independent experiments, ***P*<0.01, ****P*<0.001 (ANOVA with Bonferroni post-hoc test).

NIH-PA Author Manuscript

NIH-PA Author Manuscript

NIH-PA Author Manuscript

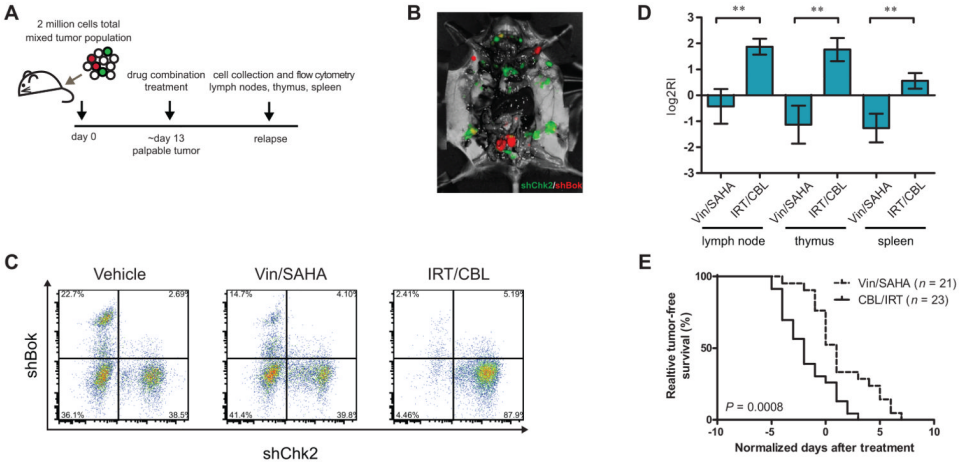

Fig. 3. *In vivo* validation of effects of combination therapies on subpopulation composition

(A) A schematic of the *in vivo* competition assay. *Eμ-Myc; p19*$^{Arf-/-}$ lymphoma cells were retrovirally transduced with desired shRNA, and mixed populations of tumor cells were tail-vein injected into recipient mice. Combination treatments were given at presentation of palpable tumor. Tumor cells were collected and analyzed at relapse. (B) Representative fluorescence imaging of vehicle-treated mice with mixed populations of parental, shChk2 (GFP-labeled), and shBok (Tomato-labeled) infected tumor cells, showing intratumoral heterogeneity *in vivo*. (C) Representative *in vivo* competition assay flow cytometry analysis of relapsed tumors following *in vivo* treatment with the indicated combination therapies. (D) An *in vivo* competition assay showing the enrichment or depletion of subpopulations of shRNA infected tumor cells. Vin/SAHA and IRT/CBL treatment data for the combined shBok and shChk2 populations are shown in lymph node, thymus, and spleen. Drug combination predictably enriched/depleted subpopulations, in agreement with *in vitro* results (Fig. 2). Data shown are mean ± s.e.m of three independent experiments (with 4-5 mice per experiment). ***P*<0.01 (two-tailed Student's t-test). (E) Relative tumor-free survival for each combination treatment on mice transplanted with heterogeneous parental/shChk2/shBok tumor, with days normalized to the median tumor-free survival of treated mice with homogeneous parental tumor. Vin/SAHA improved relative tumor-free survival when compared to IRT/CBL. Data were compiled from four independent experiments. *P* value was calculated using a log-rank test.

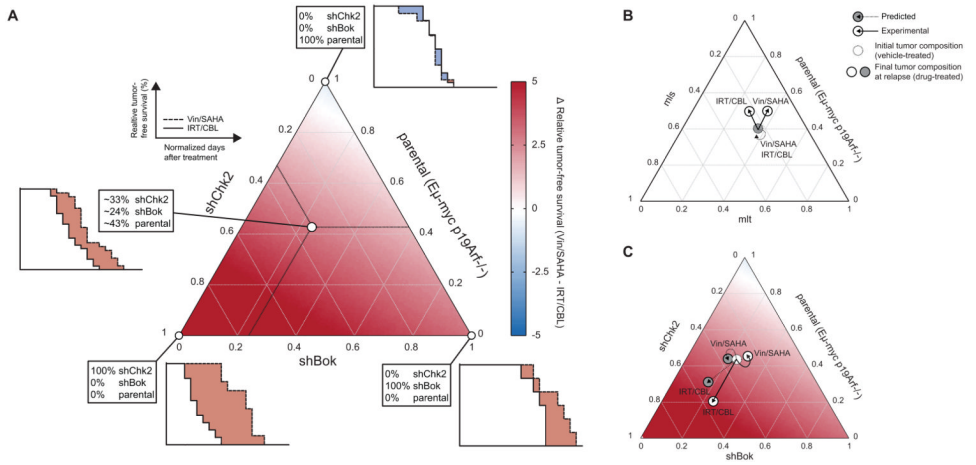

Fig. 4. Vin/SAHA is superior to IRT/CBL in extending relative tumor-free survival in a three-component heterogeneous tumor across varying subpopulation proportions

(A) A ternary plot showing the comparison between Vin/SAHA and IRT/CBL in terms of relative tumor-free survival in a shChk2/shBok/parental tumor (i.e. tumor-free survival of heterogeneous tumor normalized to that of a parental-only empty vector control) at varying subpopulation proportions. Each white dot represents a tumor composition for which experiments were performed to determine tumor-free survival in mice. Three out of the four dots at the corner of the ternary plot represents the homogeneous tumor that was used to generate the model. The position of the internal white dot approximates the heterogeneous tumor composition at the end of the experiment in vehicle-treated mice. (B-C) Predicted and actual experimental trajectories of tumor with empty vector control parental/mls/mlt (B) or heterogeneous tumor with parental/shChk2/shBok (C) upon treatment with Vin/SAHA or IRT/CBL *in vivo*. For heterogeneous tumor (C), the ternary plot was overlay with heat map in (A) showing the therapeutic efficacy comparisons between Vin/SAHA and IRT/CBL. Dotted circle denotes initial tumor composition; solid circle denotes the mean final tumor composition (of pooled lymph nodes per mouse) at relapse following treatment. Predicted trajectories are shown with gray circles and dotted arrows; experimental results of trajectories are shown in white circles and solid arrows.

NIH-PA Author Manuscript
NIH-PA Author Manuscript
NIH-PA Author Manuscript